DECEMBER 05 2002

Sound transmission across a smooth nonuniform section in an infinitely long duct

S. K. Tang; C. K. Lau

J. Acoust. Soc. Am. 112, 2602–2611 (2002)
https://doi.org/10.1121/1.1512699

Sound transmission across a smooth nonuniform section in an infinitely long duct

S. K. Tang and C. K. Lau
Department of Building Services Engineering, The Hong Kong Polytechnic University, Hong Kong, People's Republic of China

(Received 30 April 2001; revised 30 June 2002; accepted 6 August 2002)

Sound transmission across a nonuniform section in an infinite duct is studied numerically using the finite element method. An impedance matched absorptive portion is added to each end of the computational domain so as to avoid the undesirable higher mode reflection that will otherwise take place there. Results suggest that the sound fields downstream of the nonuniform section inlet are complicated and cannot be easily described by the conventional solution of the wave equation. The distribution of acoustic energy among the various propagating modes well downstream from the outlet of the nonuniform section is also discussed. Results show that the first symmetrical higher mode is important for all cases. The plane wave becomes important at high frequency with high rate of change of the cross-sectional area when the section is a convergent one. © *2002 Acoustical Society of America.* [DOI: 10.1121/1.1512699]

PACS numbers: 43.20.Mv [DEC]

I. INTRODUCTION

Ventilation and air conditioning systems are indispensable nowadays, especially in high-rise buildings within congested cities. Noise from the related building services equipment, such as the air handling unit and fans, therefore propagates into the interior of a building through the air conveying ductwork and affects directly the built environment. The conventional method for noise control is by installing dissipative silencers into the duct network.[1] Their design requires a calculation of the required noise attenuation. However owing to the complexity of the ductwork system, the present estimation procedure[2] may only provide good results at very low frequencies and lead to disappointing results once the noise frequency approaches the first cutoff of the duct, not to say at higher frequencies. The problem becomes more acute when the ductwork contains bends and sections of cross-sectional changes.

Changes of cross-sectional areas are common in an air conditioning duct network for controlling static pressure and flow velocity. Sometimes, such changes may result from a limitation of ceiling voids or the structural requirements of a building. All such variations of cross-sectional areas, or wave guides, are accompanied by acoustical impedance changes and therefore causing reflection within the ductwork. They also have their frequency characteristics and thus will act as filters.[3] The generation of, the propagation and the interactions between acoustic modes are important for optimal silencer provision as these phenomena have crucial effects on the sound transmission through the sections and the subsequent calculation for the required sound attenuation along the ductwork.

There have been a number of studies on this topic in the past few decades. Many of them are focused on the methodology of analysis. For instance, Alfredson[4] approximated the boundaries of a varying cross-section duct by a series of subsections whose sides were parallel to the duct axis and performed an investigation on the propagation of sound in an exponential horn. Also, Astley and Eversman[5] compared the use of finite element and weighted residual methods for the present issue. Besides, Nayfeh *et al.*[6] studied the sound transmission through an annular duct with variable cross-sectional area. However, the interaction of acoustic modes, the reflection and transmission of sound power in the duct are not clearly addressed. The recent work of Utsumi[7] introduces a semianalytical method for the study of sound propagation in non- uniform circular ducts. However, it is believed that a particular acoustic mode upstream of the non-uniform duct section will excite many modes in the downstream position and thus the results of Utsumi[7] appear incomplete. Also, both Utsumi[7] and Astley and Eversman[5] performed the matching at the inlet and exit of the nonuniform section where the acoustic modes may not be well developed. This problem becomes serious when the associated percentage change in the cross-sectional area is not small (cf. the vena contracta in fluid mechanics[8]) and/or the frequency of the exciting sound is high. The solution of the wave equation for straight duct section employed by Alfredson[4] and Utsumi[7] may thus not be able to describe the sound pressure fields at these critical areas. This will be further discussed later.

In the present study, the sound propagation through nonuniform two-dimensional ducts is investigated using the finite element method. Special efforts are made in examining how the nonuniform section affects the sound propagation and how the acoustic energies are redistributed at the exit of the section. In order to avoid the problem in doing matching of sound pressure and its gradient at the inlet and outlet of the nonuniform section, numerical anechoic sections are added to the computation domain. Details are given later. It is hoped that the present study can provide useful information on the acoustical properties of nonuniform duct sections and for improved duct noise control. For practical reason, only nonuniform sections that are symmetrical about the longitudinal axis will be considered.

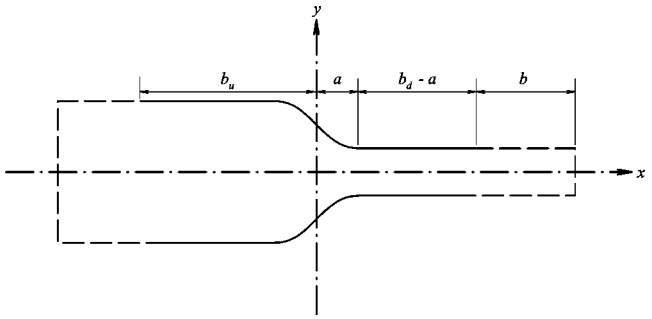

FIG. 1. Schematic diagram of the convergent section and nomenclature. —, duct boundaries; ----, anechoic termination boundaries.

II. COMPUTATIONAL DOMAINS

Effects of both convergent and divergent sections on sound transmission are investigated in the present study. The target is to solve the wave equation

$$\nabla^2 p + k^2 p = q \tag{1}$$

in the duct system, where p is the acoustic pressure, k the wave number and q the forcing. Figure 1 shows the schematic of the convergent section. The origin of the coordinate system is set to be at the center point of the nonuniform section. The forcing is applied to the system on the upstream side of the nonuniform section throughout the present investigation. Without loss of generality, the width of the narrower section is set to be unity so that all other length dimensions are normalized by this width. The wavenumber is therefore normalized by the reciprocal of this width in the foregoing analysis. The profile of the convergent section is defined by the formula

$$y = Af(x) + B, \tag{2}$$

where A and B are constants and

$$\frac{df(x)}{dx} = (x^2 - a^2)^3 \tag{3}$$

with the integration constants ignored. Expression (3) ensures the junctions between the non-uniform section and the two straight duct sections are smooth up to the second order longitudinal derivatives. A, B, and a can be adjusted to produce different convergent sections. They define the percentage change in duct width and its rate of change across the nonuniform section. The side walls are rigid so that the normal pressure gradient vanishes

$$\left.\frac{\partial p}{\partial n}\right|_{\text{wall}} = 0, \tag{4}$$

where n is the unit normal of a solid rigid boundary. In order to avoid reflections from the boundaries at the two ends of the computational domain, the boundary conditions there must be anechoic.[9] For low frequency cases where the waves in the two straight sections are planar, one can observe that for an unit strength planar sound pressure excitation to the system,

$$\frac{\partial p}{\partial n} + ikp = \begin{cases} 2ik & \text{at } x = -b_u \\ 0 & \text{at } x = b_d \end{cases}, \tag{5}$$

are the required boundary conditions. In this case, $q=0$.

However when higher modes are present, the corresponding boundary conditions are very complicated and are usually not easily implemented in the finite element computation context.[9] In the present study, anechoic terminations are introduced at the ends of the computational domain to damp down the higher modes before they reaches the end boundaries (chain lines in Fig. 1). In order to avoid reflections at the interface between an anechoic termination and the computational domain, the boundary conditions of the side walls of the former are set to be

$$\frac{\partial p}{\partial n} + ik\alpha p = 0, \tag{6}$$

where α is effectively an absorptive coefficient which varies with distance from each interface and is zero on the interface. In the present study, $\alpha = 0.01(x - b_i)^2$, where b_i is the longitudinal position of the interface, is adopted. The absorption of higher modes is very satisfactory when the length of this termination b is greater than 10. The standing wave ratio is nearly 0 dB up to $k = 6\pi$ (not shown here). The boundary condition at the exit of an anechoic termination is that for an outgoing plane wave

$$\frac{\partial p}{\partial n} + ikp = 0.$$

The unit strength planar sound pressure excitation to the system is obtained by setting

$$q = 2ke^{i\theta}\delta(x - b_u), \tag{7}$$

where δ is the delta function and θ is an arbitrary phase angle of the excitation. The latter has no bearing in the present study. Without loss of generality, θ equals $\pi/2$ in the present computations.

Unlike the matching scheme of Harari *et al.*,[10] the above computation domain enables an easy and straightforward implementation of the finite element method to solve the wave equation [Eq. (1)]. It also avoids the type of matching done by Utsumui[7] and Astley and Eversman.[5]

The computational domain for the divergent sections can be obtained by varying A, B, and a in Eqs. (2) and (3). The boundary conditions and forcing functions are again defined in the same way as those for the convergent sections and thus are not repeated here. One should note that the flow physics inside the convergent and divergent sections can be very different even if the percentage changes in cross-sectional areas of the two sections are the same. It will be shown in the next section that phenomena similar to that of the vena contracta[8] and the subsonic nozzle flows[11] can be observed at the exit of the nonuniform section provided that the percentage change in duct width and the rate of change of this width across the nonuniform section is of the right combination.

III. RESULTS AND DISCUSSIONS

For simplicity, the present investigation deals with a plane wave forcing at the upstream side of the nonuniform section. This is the case in reality as the higher mode noise is usually well attenuated some distances away from the

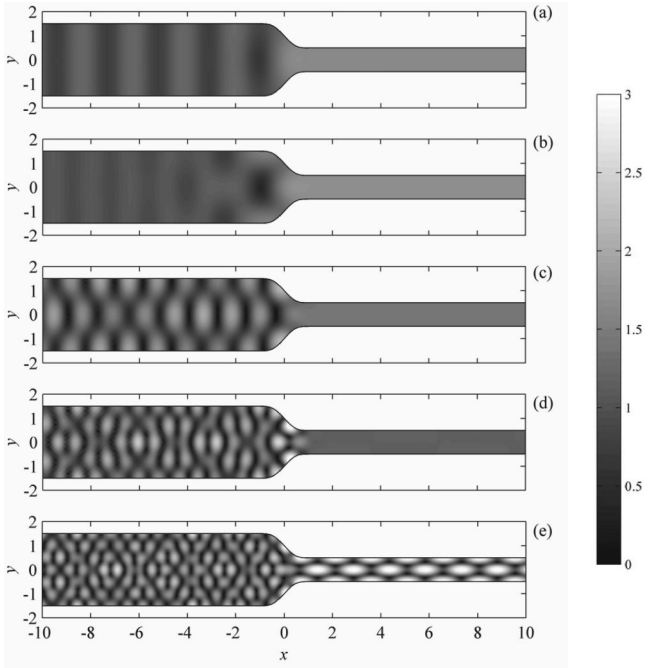

FIG. 2. Normalized sound pressure magnitude maps in the presence of a convergent section. $a=1$, $m_c=3$. (a) $k=1.5$; (b) $k=2.0$; (c) $k=3.0$; (d) $k=5.0$; (e) $k=6.5$.

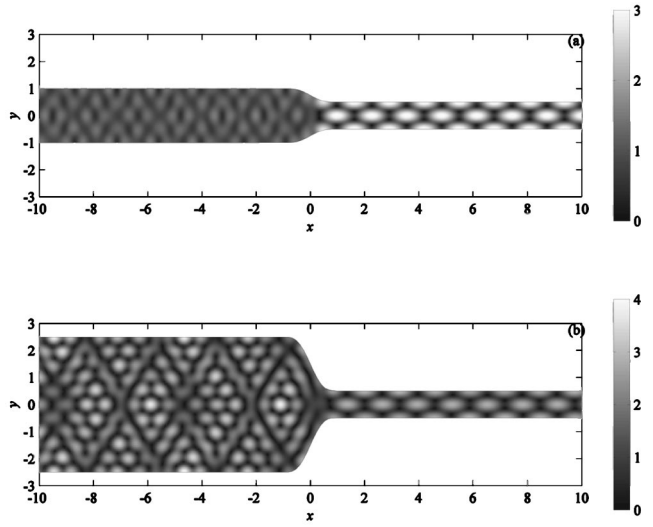

FIG. 3. Effects of convergent ratio on sound field. (a) $m_c=2$; (b) $m_c=5$. $k=6.5$, $a=1$.

source. The sound field is thus symmetrical about the longitudinal axis. Also, the present investigation is restricted at $k\leqslant 9$. One should note that the frequency with $k\leqslant 9$ is practically not high. For a duct having a width of 1 m, which is not uncommon in buildings, the first cutoff frequency of the symmetrical higher mode is only 340 Hz ($k=2\pi$). Noise from air conditioning and ventilation devices still contains significant amount of energy beyond this frequency.[1] The cutoff frequency of the second symmetrical higher mode corresponds to that with $k=4\pi$, which is high enough to be reliably attenuated by duct acoustic lining of sufficient length.

A. Convergent sections

Figure 2 shows some sound field patterns across a convergent section with $A=35/32$, $B=1.5$ and $a=1$. The convergent ratio, m_c, defined as the ratio of the larger to the smaller duct width, is 3. The sound fields for $k<1$ are not presented as the waves are almost planar even inside the convergent section. For $k=1.5$, one can note the nearly circular wave pattern at $-1<x<1$ [Fig. 2(a)]. This nonplanar (higher mode) cannot propagate back into the wider duct section as expected.[12] At $k=2$, which is close to the first symmetrical higher mode cutoff value of the wider duct section (at $k=2.09$), one can observe strong non-planar sound reflection by the convergent section [Fig. 2(b)]. The sound energy is concentrated at the walls of the section, leaving a weak sound field near the center-line. The nonplanar sound penetrates a longer distance into the upstream duct section than that at $k=1.5$ as expected.[12] At increased k beyond 2.09, the upstream sound field is made up by plane waves and the first symmetrical higher mode, while that in the downstream narrower duct is a plane wave. Figure 2(c) illustrates the sound energy distribution at $k=3$, which is typical for $2.1\leqslant k\leqslant 4$. The second symmetrical higher mode propagates into the wider duct section, while nonplanar wave pattern at the outlet of the convergent section can be observed at increased k [Fig. 2(d)]. Unlike the situation in the inlet of the convergent section, acoustic energy is concentrated at the centreline of the section outlet. This is due to the effect of vena contracta[8] where the wave is squeezed into the narrower duct section. This effect becomes more prominent as the convergent ratio increases (discussed later). For $k>6.3$, the first symmetrical higher mode propagates into the downstream without attenuation [Fig. 2(e)]. It can also be observed from Figs. 2(d) and (e) that there is a region close to the center line of the convergent section outlet where the sound pressure magnitude is very small. This is due to the higher particle velocity there under the vena contracta effect.

It can be observed that once the frequency is close to or higher than the cutoff frequency of the first symmetrical higher mode of the upstream duct section, the sound fields at the inlet and outlet of the convergent section will contain nonpropagating modes. Also, it is very clear that a plane excitation to the system will produce higher modes of substantial energy content. Therefore, the calculation of sound power transmission and reflection coefficients at a particular frequency should include all the acoustic modes involved. The analyses done by Utsumi[7] seems a bit incomplete. Besides, as the condition at the outlet of the convergent section is not equivalent to that of a straight duct section with rigid walls, the matching of solutions done by Alfredson[4] and Utsumi[7] may not be very appropriate unless the convergent ratio is close to unity. More elaboration on this point is given in the next paragraph.

At small convergent ratio, the acoustic modes are fully developed at the outlet of the convergent section [Fig. 3(a)]. However at larger convergent ratio, the flow at the outlet of the section becomes more accelerated. The higher acoustic mode may not be well developed at the convergent section outlet, especially with $k>2\pi$ [Fig. 2(e)]. Further increase in m_c makes the situation worse [Fig. 3(b)]. The convergent

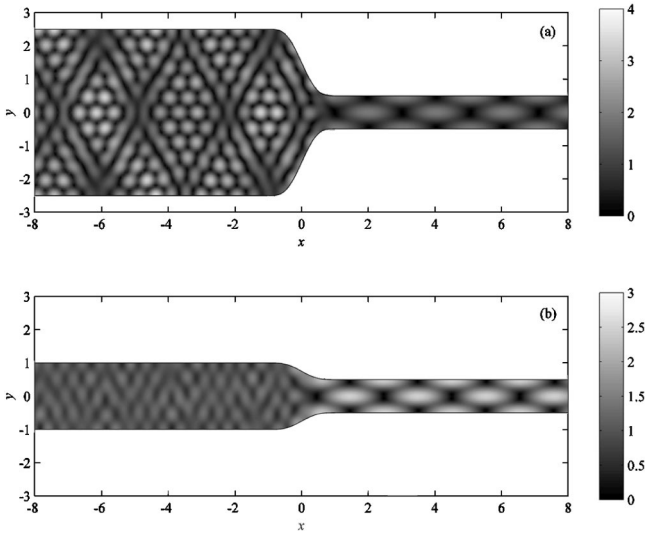

FIG. 4. Effects of convergent ratio on sound field at high frequencies. (a) $m_c=5$; (b) $m_c=2$. $k=8$, $a=1$.

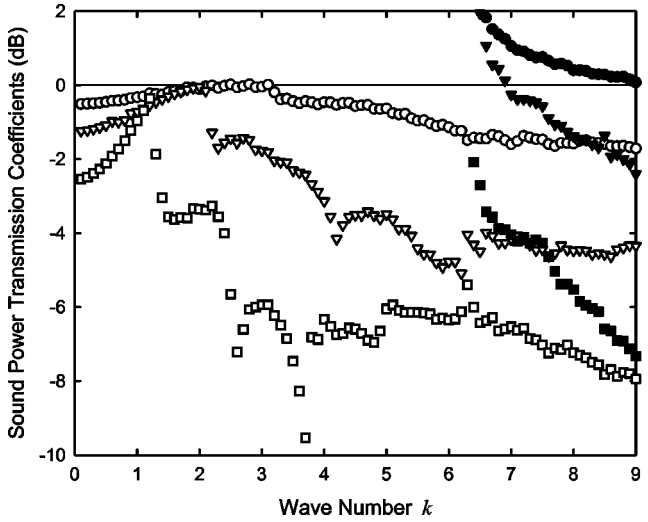

FIG. 5. Effects of convergent ratio on sound power transmission coefficients. ○, $m_c=2$; △, $m_c=3$; □, $m_c=5$. Closed symbols, total power; open symbols, plane wave power. $a=1$.

section tends to focus the sound waves and the vena contracta acts as a variable cross-section wave guide with unknown boundary condition. Such effect becomes more pronounced at higher frequencies [Fig. 4(a)]. The solution of the wave equation within this region is therefore different from that of a straight duct.[13] The technique of mode matching[4,7] may only be appropriate for small convergent ratios, where the vena contracta is located upstream of the convergent section outlet ($x<1$), so that the wave then has sufficient distance to develop before propagating into the straight duct section [Fig. 4(b)], or when the forcing frequency is sufficiently lower than the cutoff frequency of the first symmetrical higher mode of the smaller duct section.

The increase in the length of the convergent section, a, at fixed convergent ratio allows a smoother wave propagation into the smaller duct section. The effect of the vena contracta becomes weaker. Since the corresponding wave patterns look like those presented in Figs. 3 and 4, they are not presented here. However, it will be shown later than this length has substantial effects on the sound transmission process.

Figure 5 illustrates the variations of the overall sound power transmission coefficient τ_0 and the plane wave power transmission coefficient τ_p with the forcing frequency respectively for $m_c=2$, 3, and 5 with $a=1$. The latter refers to the ratio of the power carried by the plane wave downstream of the convergent section to that of the incident power. One can easily realize that $\tau_0=\tau_p$ for forcing frequencies below the cutoff frequency of the first symmetrical higher mode of the smaller duct section. The corresponding limiting value of τ_0 at $k\rightarrow 0$ $(=\tau_p)$, can be calculated using the plane wave theory with abrupt contraction.[3] For the convergent ratios of 2, 3, and 5, these values are 0.89, 0.75, and 0.56, respectively.

One can observe from Fig. 5 for $k<6.3$ that τ_0 increases as the forcing frequency approaches the cutoff frequency of the first symmetrical higher mode of the larger duct section for all m_c. The overall sound power transmission coefficient can be very close to 1. This can also be predicted using the classical plane wave calculation. At very low frequency, the length of the convergent section is very small when compared to the wavelength of the sound. The sound wave thus sees the section as an abrupt contraction. As frequency increases, the rate of contraction seen by the wave becomes lower and thus τ_0 increases as higher percentage of the incident sound power can propagate through the section. The maximum sound power transmission coefficient depends on the smoothness of the convergence. It is expected that the smoother the convergence, the closer it will be to unity.

At frequency increases beyond that of the first symmetrical higher mode of the larger duct section, higher mode propagates back to the upstream [Fig. 2(c)] and thus the power carried by the transmitted plane wave becomes less. A drop of τ_0 then follows. The τ_0 in general decreases as k further increases towards 6.3. Such phenomenon can also be predicted using the classical plane wave calculation[3] (not shown here). However, large dips of τ_0 are observed close to the cutoff frequencies of the symmetrical higher modes of the larger duct section for all m_c investigated in general. This situation becomes more acute as m_c increases. At these frequencies, the reflected waves, having the wavelength in the transverse direction greater than 1, are strong and carry substantial amount of energy under resonance. Figure 6(a) shows a typical example with $m_c=5$, $a=1$, and $k=3.7$. This phenomenon is not reported by Utsumi.[7] It should be noted that the results of Utsumi[7] are related to transmitted wave magnitudes, not the sound power transmitted. It can be noted that a dip of τ_0 is not observed at $k\sim 5$ for $m_c=5$, while the corresponding forcing frequency is close to that of the fourth symmetrical higher mode of the larger duct section ($k=5.03$). At this frequency, the transverse wavelength of the reflected sound is about 0.63. The reflection is therefore not strong [Fig. 6(b)].

For $k>2\pi$, higher mode propagates along the smaller duct section and $\tau_0>\tau_p$. Large transmitted sound power is found at $k=6.3$ for all values of m_c investigated. The corre-

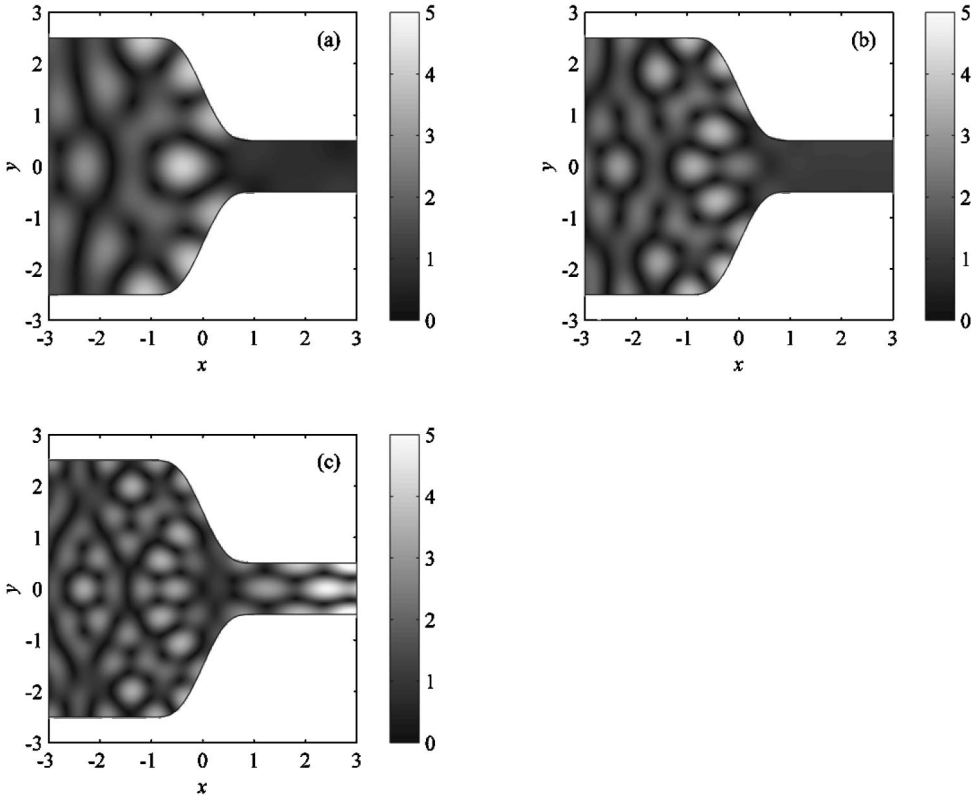

FIG. 6. Sound fields close to convergent section outlet. (a) $k=3.7$; (b) $k=5$; (c) $k=6.3$. $m_c=5$, $a=1$.

sponding forcing frequency is very close to that at which resonance can occur in both straight duct sections (wave number $k=2\pi$). Most of the transmitted sound power is carried downstream by the first symmetrical higher mode propagating in the smaller duct section as illustrated in Fig. 5. The strong higher mode propagation in the downstream direction suggests low impedance for sound propagation at the outlet of the convergent section. The corresponding pressure magnitude at this location is therefore, unlike those shown in Figs. 6(a) and (b), weak. An example of this is given in Fig. 6(c). This suggests that the overall sound power carried by the reflected waves is out-of-phase to that in the smaller duct section. As expected, a further increase of k results in lower magnitude of the symmetrical higher mode in the smaller duct section. One expects another strong rise of τ_0 above 1 at $k=4\pi$; the wave number corresponds to the cut-off frequency of the second symmetrical higher mode of the smaller duct section.

Increasing the length of the convergent section (that is, increasing a) reduces the magnitude of the dip at duct eigenfrequencies as shown in Fig. 7. For $a>1$, its effect is similar to that of reducing the convergent ratio. The smooth convergence offers a slow impedance change across the convergent section and thus helps avoiding strong reflection even close to the first and second symmetrical higher mode cutoff frequencies of the larger duct section. The convergence becomes rapid as a is reduced. For $a=1/\pi$ ($a\sim0.32$), the wave sees the convergent section as an abrupt contraction for $k\leqslant2$ (Fig. 7). Strong dips of τ_0 can also be observed at similar values of k as for the case of $a=1$, but an additional dip is observed at $k\sim2.9$. The sound fields at $k=2.4$, 2.8, 2.9, and 3.3 shown in Fig. 8 suggest relatively higher concentration of acoustic energy at the edges of the convergent section at k around 2.8 and 2.9. Such τ_0 dip is absent for $a\geqslant1$ (Figs. 5 and 7). It is very likely to be due to the resonance inside the convergent section. If one simplifies this section as a straight taper convergent wave guide having a slope equals to the average slope of the present convergent section, which is -1.72 for $a=1/\pi$ and $m_c=3$, one will find the first even angular mode inside such wave guide resonates at $k\sim3$ (Appendix). Such resonance produces high impedance and strong reflection in form of higher mode back to the upstream. Similar resonance also occurs at $k\sim6$ (not shown

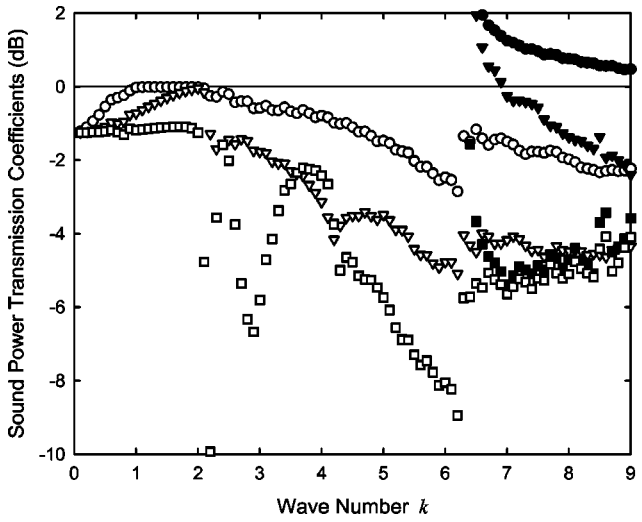

FIG. 7. Effects of convergent section length on sound power transmission coefficients. ○, $a=2.75$; △, $a=1$; □, $a=1/\pi$. Closed symbols, total power; open symbols, plane wave power. $m_c=3$.

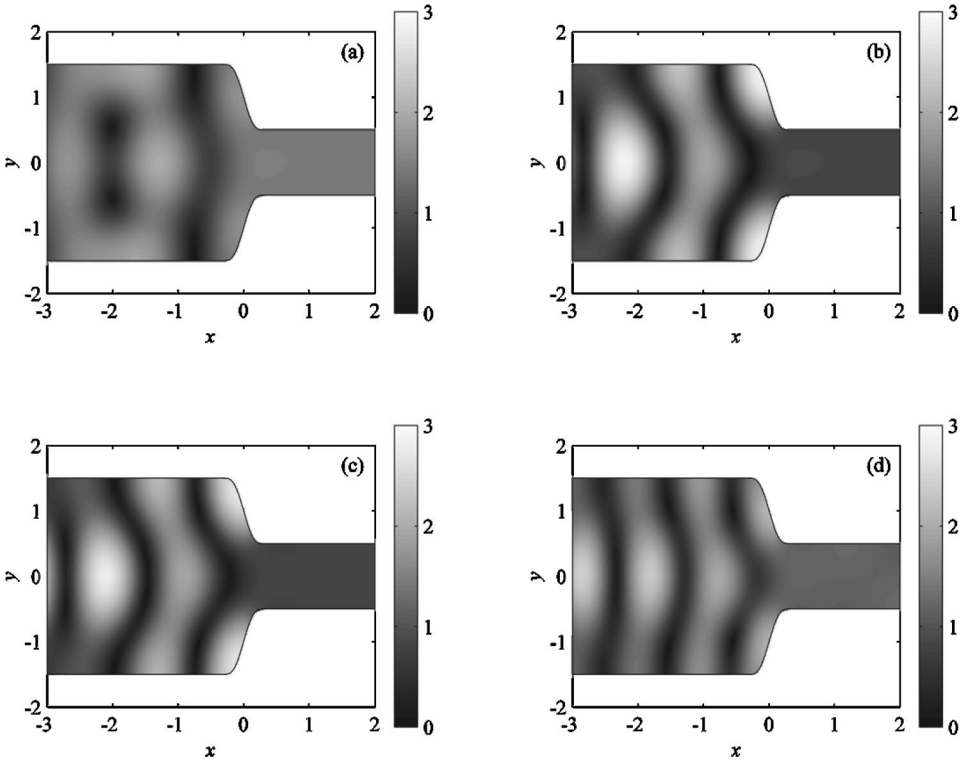

FIG. 8. Reflection of sound by convergent section at weak sound power transmission. (a) $k=2.4$; (b) $k=2.8$; (c) $k=2.9$; (d) $k=3.3$. $m_c=3$, $a=1/\pi$.

here). This effect is not found for $a=1$ or 2.75 because the corresponding wave number will be higher than 6.3. However, further investigation is necessary for clarifying the issue.

Again, resonance occurs at $k\sim6.3$ for all values of a investigated (Fig. 7). One can also observe that at small a, the plane wave in the smaller duct section carries more energy than the higher modes. The rapid contraction appears to have impeded the development of the higher mode inside the smaller duct section. The opposite is observed at large a.

B. Divergent sections

The flow across a divergent section is completely different from that across a convergent one. The divergent ratio m_d is defined as the ratio between the widths of the downstream and upstream straight duct sections. Figure 9 illustrates that the flow, with $a=1$ and $m_d=3$, is rather similar to that issuing from a subsonic nozzle,[11] when the forcing frequency is higher than the first symmetrical higher mode of the downstream larger duct section. The application of the mode matching technique for solving the present sound propagation problem as in Utsumi[7] appears questionable. Figure 9(a) suggests the high impedance of the divergent section to sound propagation at low frequencies. One can find strong reflection and standing wave patterns at these frequencies. Above the first symmetrical higher mode cutoff frequency of the larger duct section, the impedance becomes weak [Fig. 9(b)] and one can observe from Fig. 9(c) that nearly all the incident wave energy is transmitted across the divergent section. It will be further discussed later. Higher mode reflection is observed at $k>6.3$ as expected.

One can also notice from Fig. 9 that the mode patterns in the larger duct section are less ordered than those observed previously with convergent sections (Fig. 2 for instance) at high frequencies. More intensive low energy (pressure magnitude) lines and regions are found as the forcing frequency increases. This is probably due to the destructive interference from various acoustic modes inside the larger duct section. However, the patterns of these lines and/or regions do not follow any well-defined mode shapes. There are two thin low

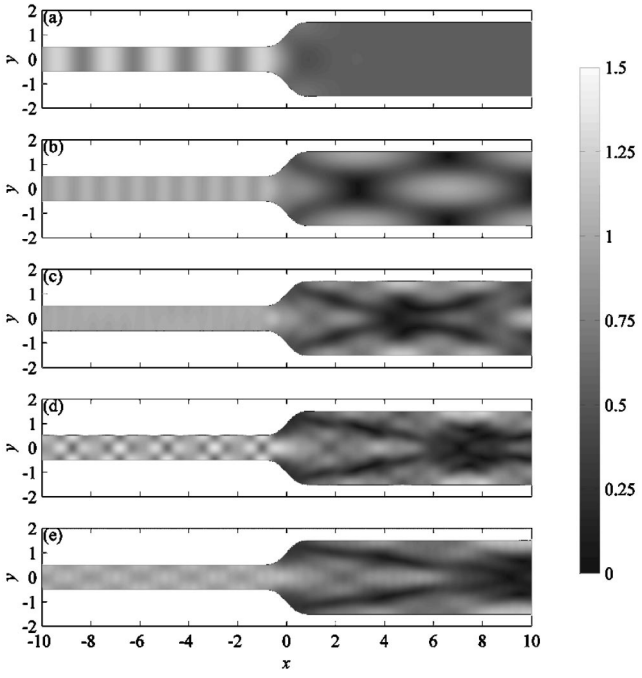

FIG. 9. Sound magnitude maps in the presence of a divergent section. (a) $k=1.5$; (b) $k=3$; (c) $k=5$; (d) $k=6.5$; (e) $k=8$; $a=1$, $m_d=3$.

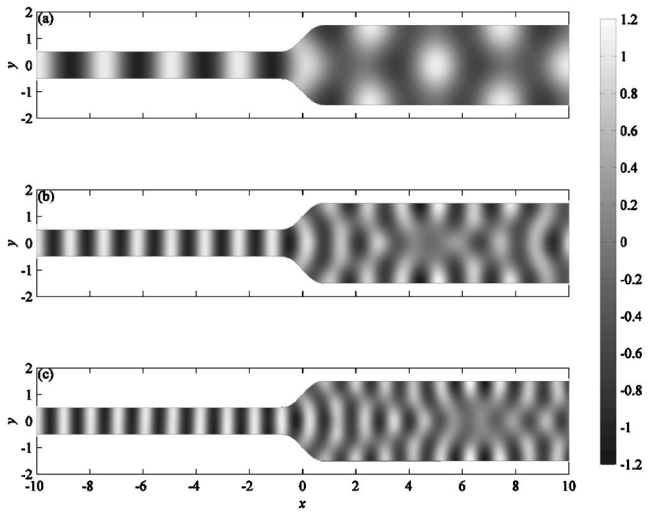

FIG. 10. Transition of sound waves into higher modes through a divergent section. (a) $k=2.5$; (b) $k=5$; (c) $k=6.2$. $a=1$, $m_d=3$.

energy regions (lines) close to the outlet of the divergent section. These regions intersect at some distances downstream of the outlet, forming a boundary, which looks like that of the potential core in a subsonic jet.[11] The wave fields close to the divergent section outlet suggest the breakup of the nearly circular wave fronts into higher duct mode patterns at frequencies higher than that of the first symmetrical higher mode of the larger duct section (Fig. 10). The lines of low energy correspond to nodal locations. The fluid velocity within the region enclosed by the two strong low energy lines close to the divergent section outlet (the potential core) appears to be higher than those outside the region; a phenomenon commonly found in the initial region of a subsonic jet.[11] A phase difference exists between waves inside and outside the potential core. The patterns of the sound fields there thus cannot be represented by the mode shapes of the straight duct section.

The variations of m_d and a certainly affect the sound transmission processes. One can find more complicated networking of the low energy lines and regions as the rate of divergence increases (m_d increases or a decreases). However, more energy is concentrated within the potential core region at increased rate of divergence. Figure 11 gives some ideas on such phenomenon. Though the sound fields inside the larger straight duct section are complicated, one can still expect that there exist plane waves in this duct section as the transverse pressure distributions have non-vanishing mean values at a distance beyond the potential core where the flow is expected to have fully developed (not shown here). One can also expect the coexistence of many acoustic modes.

Figure 12(a) shows the energy contents of the acoustic modes well downstream from the divergent section outlet for $m_d=3$ and $a=1$ at various forcing frequencies. Only plane waves are found inside the duct at forcing frequencies below the first cutoff frequency of the symmetrical higher mode of the larger duct section and thus $\tau_0=\tau_p$. Resonance occurs at $k\sim2.09$. A rise in the first symmetrical higher mode power is resulted. It is accompanied by a fall of the plane wave power. Such phenomenon is expected to have occurred in the presence of convergent sections, but the resonance takes place in the upstream side. A dip of τ_0 (or τ_p) in Figs. 5 and 7 should be accompanied by a rise of the overall reflected wave power. The cutoff frequency of the second symmetrical higher mode of the larger duct section corresponds to a wave number $k\sim4.18$. It is found that such resonance results in a redistribution of energy from the plane wave to the symmetrical higher modes. The first symmetrical higher mode

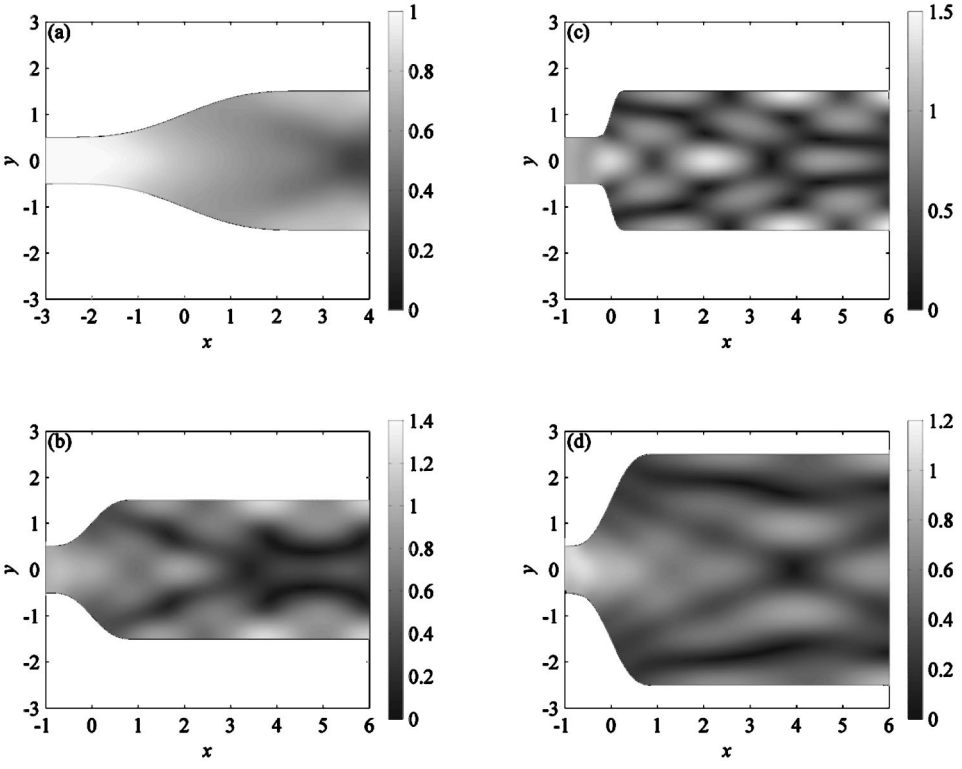

FIG. 11. Effects of rate of divergence on sound field immediate downstream of divergent section. (a) $a=2.75$, $m_d=2$; (b) $a=1$, $m_d=3$; (c) $a=1/\pi$, $m_d=3$; (d) $a=1$, $m_d=5$; $k=4.5$.

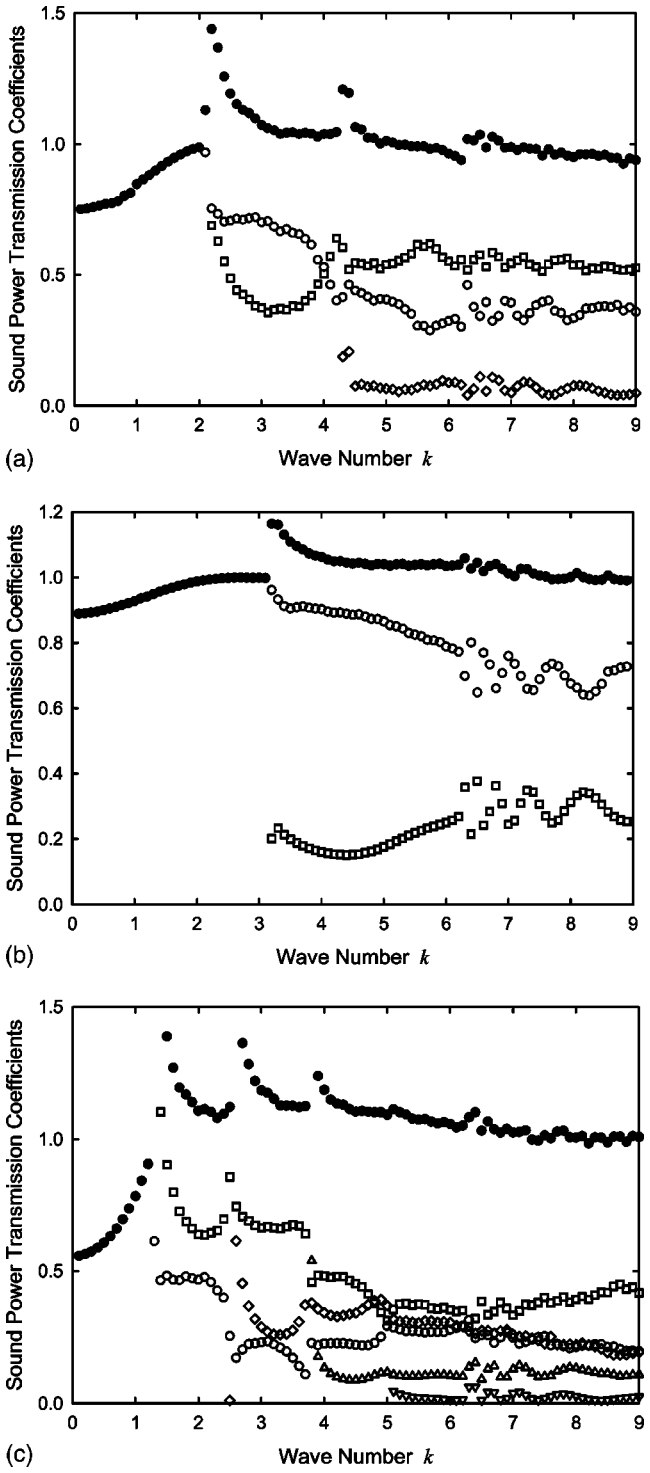

FIG. 12. Variations of sound power transmission coefficients with forcing frequency for divergent section. (a) $m_d=3$; (b) $m_d=2$; (c) $m_d=5$. ●, total; ○, plane wave; □, first symmetrical higher mode; ◇, second symmetrical higher mode; △, third symmetrical higher mode; ▽, fourth symmetrical higher mode.

becomes the dominant one for $k\geqslant 4.2$. A sharp drop of plane wave power is thus explained. Resonance is also observed at $k\sim 6.3$ as expected. The powers carried by the fourth and fifth symmetrical higher modes are negligible and thus are not presented.

At lower divergent ratio, less number of acoustic modes will be excited at $k<9$ [Fig. 9(b)]. At $m_d=2$, the only significant waves that are propagating downstream are the plane wave and the first symmetrical higher mode. The plane wave basically dominates the sound field downstream of the divergent section. However at increased m_d, the first symmetrical higher mode becomes dominant when the forcing frequency is above its cutoff frequency [Fig. 12(c)]. Again as has been observed in Fig. 12(a), the resonance at the cutoff frequency of the second symmetrical higher mode results in a decrease of the plane wave power but also an increase in the power carried by the first symmetrical higher mode. The resonance at $k\sim 3.7$ of the third symmetrical higher mode produces a drop of the first symmetrical higher mode power but a rise of that of the plane wave mode. It is also observed that the plane wave energy becomes more comparable to those of the first and second symmetrical higher modes as k increases further. The on-set of the third and the fourth higher modes results in a redistribution of energy back to the plane wave mode. The reason is left to further investigations.

Results shown in Fig. 12 tend to suggest that the on-set of a symmetrical higher mode propagation in the larger duct section, except for the case of the first symmetrical higher mode which must take energy from the plane wave, is usually followed by a drop of the power carried by an acoustic mode two orders lower than this mode for $k\leqslant 6.2$. Also, one can observe large fluctuations of sound transmission coefficients for $k>6.3$. These fluctuations become smoother as the forcing frequency increases. However at small m_d, for example $m_d=2$, these fluctuations associated with the plane wave and the first symmetrical higher mode vary out of phase with each other in this k range [Fig. 12(b)]. Similar phenomena are expected also at larger m_d between various propagating acoustic modes, but the data would be difficult to interpret as the energy is distributed among several of these modes. The reason for the occurrence of these fluctuations is not exactly known. However, one can expect from the duct acoustics theory[14] that it is due to the form of excitation to the acoustic modes in the larger duct section. If one looks at the acoustic pressure magnitude distribution close to the nonuniform section as shown in Fig. 13, it is found that the energy is more widely spread across the inlet of the divergent section for $k=7$ and 7.7 than for $k=6.8$ and 7.3. The excitation at $k=7$ or 7.7 is therefore more uniform across the duct section and thus higher plane wave energy content can be anticipated. For $k=6.8$ or 7.3, more energy will then be redistributed to the higher mode. One can observe that it is due to the phase of the higher mode reflected back into the smaller duct section. The input impedance of the divergent section thus plays an important role for the occurrence of this phenomenon. One also expects that this impedance varies across the cross section of the divergent section inlet. Though there are studies concerning the input impedances of wave guides (for instance, Ref. 15), results related to the present type of cross sectional change are not easily found in existing literature. Further investigation is required. Similar observations as in Figs. 12 and 13 can be made when a is varied. The corresponding results are thus not presented.

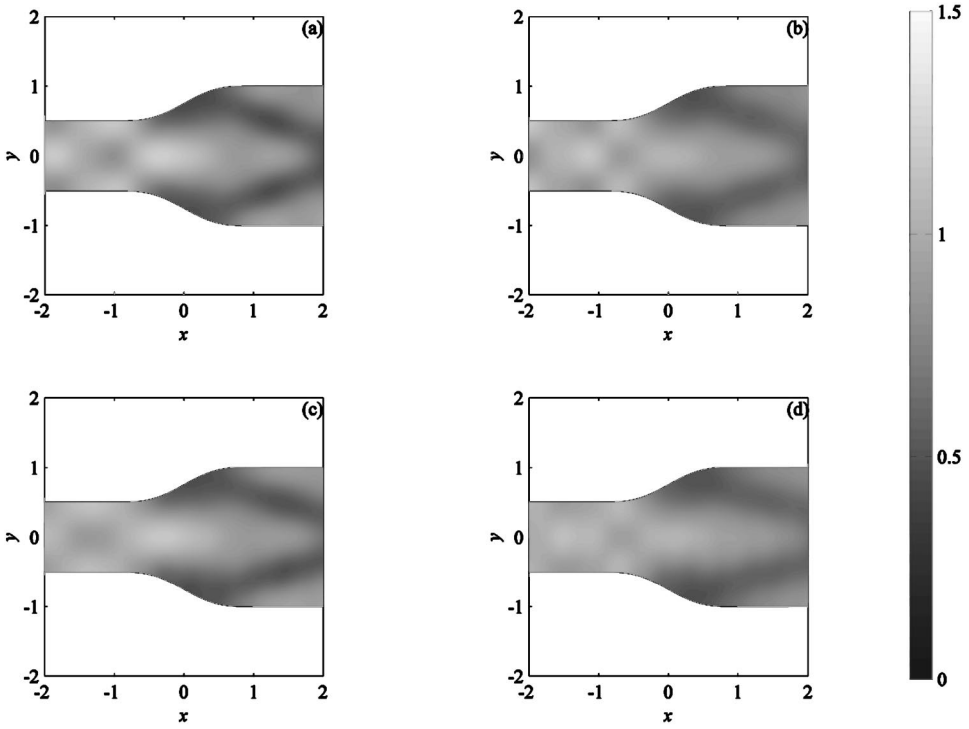

FIG. 13. Spreading of sound waves across divergent section at high frequencies. (a) $k=6.8$; (b) $k=7$; (c) $k=7.3$; (d) $k=7.7$. $a=1$, $m_d=2$.

IV. CONCLUSIONS

The sound transmission across a nonuniform section in an infinite duct is investigated by using the finite element method. Special absorption boundaries are included in the computational domains in order to avoid the erroneous reflection from the ends of the domains. The excitation is taken to be a plane wave. For practical reasons, only symmetrical divergent and convergent sections are considered in the present study. The sound field patterns and the distributions of energy among the different propagating acoustic modes under various forcing frequencies are also discussed.

Results obtained with convergent sections illustrate that there are regions of high energy content close to the center line of the section outlet when the forcing frequency is higher than the first symmetrical higher mode of the larger duct section. The situation becomes more serious as the forcing frequency increases. This is probably due to the nonparallel fluid flow near the convergent section outlet at higher frequencies. The sound power transmission coefficient increases with forcing frequency before the first symmetrical higher mode is reflected back into the larger duct section. The power carried by the transmitted plane wave decreases as the forcing frequency increases beyond the cutoff frequency of this mode in general. Sharp drop of plane wave power is found when the forcing frequency collapses with the eigenfrequencies of the larger duct section. High transmitted sound energy is observed at forcing frequencies close to the first symmetrical higher mode eigenfrequency of the smaller duct section. It is also found that the higher the rate of convergence, the lower the overall sound transmission coefficient. Besides, it is observed that the first symmetrical acoustic mode dominates the final sound field inside the smaller duct section at high frequency, unless the rate of convergence is sufficiently high.

The sound fields in the presence of a divergent section are more complicated. At a forcing frequency higher than the first symmetrical higher mode of the downstream larger duct section, the transmitted energy is concentrated on the center line within or at a location slightly downstream of the divergent section. The walls of the divergent section are usually under a weak pressure condition. The sound energy distribution pattern downstream of the inlet of the divergent section resembles that of a subsonic jet velocity field. Again, large energy content of a particular propagating mode is observed when the forcing frequency is close to its cutoff frequency. The distribution of acoustic energy among the propagating modes in the fully developed region inside the larger duct section suggests that the first symmetrical higher mode carries higher energy content than the other propagating modes once it is excited. The plane wave will only be more important when the rate of divergence is low or the forcing frequency is not high. It is also found that the impedance offered by the divergent section is important for the final distribution of energy among the propagating modes downstream of the section.

ACKNOWLEDGMENT

This study is supported by a grant from the Research Grant Council, The Hong Kong Special Administration Region Government, People's Republic of China.

APPENDIX: ANGULAR MODES IN A SYMMETRICAL TAPER SECTION

The sound field inside a symmetrical taper section (Fig. 14) is best to be obtained by solving the wave equation in polar coordinate (r, ϕ);

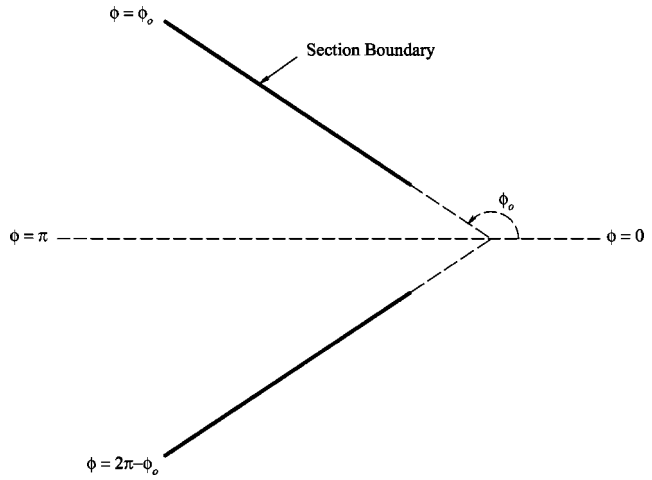

FIG. 14. Schematic diagram of a symmetrical linear taper section.

$$\nabla^2 p + k^2 p = \frac{\partial^2 p}{\partial r^2} + \frac{1}{r}\frac{\partial p}{\partial r} + \frac{1}{r^2}\frac{\partial^2 p}{\partial \phi^2} + k^2 p = 0. \tag{A1}$$

The method of separation of variables suggests the solution is

$$p(r,\phi) = R(r)\Phi(\phi), \tag{A2}$$

where R and Φ are sole functions of r and ϕ, respectively. Let $k\phi$ be a positive number and $rk > k_\phi$, the angular mode of the solution Φ can be obtained by solving

$$\frac{\partial^2 \Phi}{\partial \phi^2} + k_\phi^2 \Phi = 0, \tag{A3}$$

with the hard wall boundary condition $\partial\Phi/\partial\phi_{\phi=\phi_0} = \partial\Phi/\partial\phi_{\phi=2\pi-\phi_0} = 0$. One finds

$$k_\phi = \frac{m\pi}{2(\pi - \phi_0)} \tag{A4}$$

and

$$\Phi(\phi) = \cos(k_\phi(\phi - \phi_0)), \tag{A5}$$

where m is an integer. A taper slope of -1.72 corresponds to $\pi - \phi_0 \approx 1.044$ and the first symmetrical angular mode ($m=2$) resonates at $k = k\phi \sim 3$.

[1] C. M. Harris, *Handbook of Noise Control* (McGraw-Hill, New York, 1979).
[2] D. D. Reynolds and J. M. Bledsoe, *Algorithms for HVAC Acoustics* (ASHRAE, 1991).
[3] L. E. Kinsler and A. R. Frey, *Fundamentals of Acoustics* (Wiley, New York, 1962).
[4] R. J. Alfredson, "The propagation of sound in a circular duct of continuously varying cross-sectional area," J. Sound Vib. **23**, 433–442 (1972).
[5] R. J. Astley and W. Eversman, "A finite element method for transmission in non-uniform ducts without flow: Comparison with the method of weighted residuals," J. Sound Vib. **57**, 367–388 (1978).
[6] A. H. Nayfeh, J. E. Kaiser, R. L. Marshell, and C. J. Hurst, "A comparison of experiment and theory for sound propagation in variable area ducts," J. Sound Vib. **71**, 241–259 (1980).
[7] M. Utsumi, "An efficient method for sound transmission in nonuniform circular ducts," J. Sound Vib. **227**, 735–748 (1999).
[8] V. L. Streeter and E. B. Wylie, *Fluid Mechanics* (McGraw-Hill, Singapore, 1983).
[9] A. Bayliss and E. Turkel, "Far field boundary conditions for compressible flows," J. Comput. Phys. **48**, 182–199 (1982).
[10] I. Harari, M. Slavutin, and E. Turkel, "Analytical and numerical studies of a finite element PML for the Helmholtz equation," J. Comput. Acoust. **8**, 121–137 (2000).
[11] A. K. M. F. Hussain and A. R. Clark, "On the coherent structure of axisymmetric mixing layer: A flow visualization study," J. Fluid Mech. **104**, 263–294 (1981).
[12] P. M. Morse and K. U. Ingard, *Theoretical Acoustics* (McGraw-Hill, New York, 1968).
[13] M. Razavy, "An acoustic waveguide with variable cross section," J. Acoust. Soc. Am. **86**, 1155–1160 (1989).
[14] P. E. Doak, "Excitation, transmission and radiation of sound from source distributions in hard-walled ducts of finite length (I): The effects of duct cross-section geometry and source distribution space-time pattern," J. Sound Vib. **31**, 1–72 (1973).
[15] N. Amir, V. Pagneux, and J. Kergomard, "A study of wave propagation in varying cross-section waveguides by modal decomposition. Part II. Results," J. Acoust. Soc. Am. **101**, 2504–2517 (1997).